Removing the "heavy mineral effect" to obtain a new Pb isotopic value for the upper crust

Marion Garçon, Catherine Chauvel, Christian France-Lanord, Mara Limonta, Eduardo Garzanti

Geochemistry, Geophysics, Geosystems
DOI 10.1002/ggge.20219

Removing the "heavy mineral effect" to obtain a new Pb isotopic value for the upper crust

Marion Garçon[1*], Catherine Chauvel[1], Christian France-Lanord[2], Mara Limonta[3], Eduardo Garzanti[3]

[1] ISTerre, Université de Grenoble 1, CNRS, BP 53, 38041 Grenoble Cedex 09, France

[2] CRPG-CNRS, 15, rue Notre Dame des Pauvres, 54501 Vandoeuvre-lès-Nancy, France

[3] Laboratorio di Petrografia del Sedimentario, Dipartimento di Scienze Geologiche e Geotecnologie, Università di Milano-Bicocca, 20126 Milano, Italy

* Corresponding author
e-mail: marion.garcon@ujf-grenoble.fr

Received: Feb 20, 2013; Revised: Jul 01, 2013; Accepted: Jul 02, 2013

KEY POINTS

- **Large Pb isotopic variability in river sediments due to mineral sorting processes**
- **Pb isotopes of river sediments are biased by a heavy mineral effect**
- **New average Pb isotopic values for Himalayan crust and upper continental crust**

KEYWORDS : Pb isotopes, sediment, mineral, Himalaya, continental crust

ABSTRACT

Based on the concept that sedimentary processes average large areas of exposed crust, sediment data have been widely used to estimate the average Pb isotopic composition of the upper continental crust. However, the possible effects of mineral sorting processes on sediment Pb isotopes have never been fully investigated. Here, we report Pb isotopic compositions of Himalayan river sediments as well as those of several grain-size fractions and mineral separates. We demonstrate that Pb isotopes of both bedloads and suspended loads are biased towards more radiogenic values than their source rocks due to a "heavy mineral effect" caused by mineral sorting during fluvial transport on continents. The sparse zircons, monazites and allanites present in all samples (<1wt%), including suspended loads, generate a Pb isotopic variability as large as that observed in the Earth's mantle. After correction of this effect, we propose an average value for the composition of the upper Himalayan crust together with a new Pb isotopic value for the Earth's upper continental crust. We conclude that mineralogical effects must be evaluated carefully before using Pb isotopes of sediments as provenance and anthropogenic tracers.

1. INTRODUCTION

Knowing the average Pb isotopic composition of the continental crust is crucial to constrain the evolution of the Earth since its formation. Current estimates are rare. Some come from Earth evolution models [*Kramers and Tolstikhin, 1997*; *Zartman and Doe*, 1981] but most are based on data acquired from river or oceanic sediments [*Asmerom and Jacobsen*, 1993; *Allègre et al.*, 1996; *Millot et al.*, 2004]. The latter assume that sediments are representative of their continental sources but bias can be introduced if sedimentary mineral sorting is ignored. *Patchett et al.* [1984] demonstrated that Hf isotopes are fractionated by the so-called "zircon effect", i.e. preferential concentration of unradiogenic Hf-rich zircons in coarse sediments which produces finer sediments with much more radiogenic Hf isotopes than their continental sources. Because heavy minerals have sometime extremely radiogenic Pb isotopes, here, we evaluate the impact of the "heavy mineral effect" on Pb isotopes of river sediments. We used a comprehensive set of samples including bedloads, bank sediments and suspended loads sampled in the Ganga and its major tributaries draining the Himalayan mountain range together with several grain-size fractions and 12 mineral separates isolated from some of these sediments. Using all these data, we demonstrate that mineral sorting processes during fluvial transport bias the sedimentary record and generate a large Pb isotopic variability. We quantify this effect and suggest an alternative to properly estimate the sediment source compositions. Finally, we estimate an average Pb isotopic composition for the upper Himalayan crust and propose a new Pb isotopic value for the Earth's upper continental crust.

2. CONTEXT AND SAMPLES

The Ganga is one of the largest river on Earth, delivering annually ca. 400 million tons of sediments to the Bay of Bengal [*Lupker et al.*, 2011]. Because of its critical role in the world's sedimentation system [*Milliman and Meade*, 1983], this fluvial network constitutes

an excellent laboratory to assess the global isotopic systematics of river sediments. The Ganga fluvial system essentially carry the erosion products of the Himalayan orogenic belt which can be divided into four main geological units from north to south [*Le Fort*, 1975] : (1) the variably metamorphosed sedimentary rocks of the Tethyan Sedimentary Series, (2) the highly metamorphosed crystalline rocks of the High Himalayan Crystalline, (3) the weakly metamorphosed sedimentary rocks of the Lesser Himalaya, and (4) the Siwaliks made of Neogene to Quaternary floodplain deposits (Figure 1).

In this paper, we report Pb isotopes of (a) sediments carried by Himalayan rivers draining monolithologic catchments in the mountain range, and (b) bedload, bank and suspended load sediments sampled in the floodplain at the Himalayan front and further downstream in the Ganga and its major tributaries. To understand what controls Pb isotopes in river sediments, we also analyzed pure separates of biotite, K-feldspar, muscovite, plagioclase, magnetite, epidote, titanite, vermiculite, amphibole, carbonate and one fraction enriched in zircon, monazite and allanite separated from a bedload sampled at the outflow of the Ganga, as well as several grain-size fractions separated from a suspended load and a bank sediment.

3. METHODS

Sampling techniques for bedloads, bank sediments and suspended loads can be found in *Galy et al*.[2008] and *Lupker et al.*[2011]. Grain-size fractions were separated from two samples (PB 60 and BGP 6) by sieving and settling techniques. Mineral separates were obtained from different grain-size fractions of sample BR 717. We used successive centrifugations in sodium metatungstate and methylene iodide to separate the minerals as a function of their densities and recovered them by partial freezing in liquid nitrogen. Each mineral separate was then carefully purified under the binocular microscope. Unfortunately, we could not isolate pure zircon, monazite and allanite fractions because the grains were too small to be

handpicked under the binocular microscope. Instead, we separated all the heavy minerals (density>3.3 $g.cm^{-3}$) from the 2-63μm fraction of BR 717 and analyzed this heavy mineral concentrate, which is highly enriched in zircon, monazite and allanite as demonstrated by the petrologic and chemical studies conducted by *Garzanti et al.*[2010; 2011] on samples collected at the same location. 5 to 10 mg mineral separates and 50 to 100 mg powder for both bulk sediments and grain-size fractions were dissolved for 2 days in HNO_3 14N on a hot plate at 130°C prior to be evaporated and further digested in a mixture of HF and $HClO_4$ in teflon containers placed in steel PARR bombs for 6 weeks at 140°C or one week at 200°C. Following the analytical procedure described by *Chauvel et al.*[2011], the isolation of Pb was carried out with anion AG1-X8 resin. Pb isotopic ratios were measured on a Nu Plasma MC-ICP-MS at ENS Lyon (France). Mass fractionation bias was corrected using a thallium spike [*White et al.*, 2000]. Analytical drift was corrected by the standard bracketing technique using the measured values for the NBS 981 standard run every two or three samples and those published by *Galer and Abouchami* [1998]. The reproducibility (1σ) of our measurements for the NBS 981 standard, measured 66 times, is better than 270 ppm for $^{208}Pb/^{204}Pb$, 180 ppm for $^{207}Pb/^{204}Pb$ and 420 ppm for $^{206}Pb/^{204}Pb$. Total procedural blanks average 280 pg and are always negligible relative to the amount of Pb isolated in each sample.

4. RESULTS AND DISCUSSION

4.1 What causes the Pb isotopic diversity?

Pb isotopic compositions of river sediments sampled in the Himalayan mountain range and in the floodplain are provided in Supplementary Table 1 and shown in Figure 2. *Lupker et al.* [2012] provide major element data on the same samples and *Garçon* [2012] and *Garçon et al.*[2011] report trace elements and Nd-Hf isotopes. The most striking feature seen in Figure 2 is that Himalayan sediments define a remarkable linear trend in Pb isotopic

spaces, spanning an extremely large range of values compared to that known for terrestrial rocks. Such a linear array in Pb diagrams is puzzling: it could be interpreted as an isochron but because Nd isotopes of Himalayan river sediments and U-Pb ages of individual zircons demonstrate that the sources of sediments are diverse and have different ages [*Parrish and Hodges*, 1996; *DeCelles et al.*, 2000; *Richards et al.*, 2005], this is very unlikely. Alternatively, the trend could result from mixing of sediments derived from Himalayan sources with different Pb isotopic signatures. We also reject this interpretation because sediments eroded from single geological units have extremely variable Pb compositions and do not define end member values along the array. For example, sediments eroded from the Lesser Himalaya units, which include much older rocks than the other geological units [*Parrish and Hodges*, 1996; *DeCelles et al.*, 2000], do not exhibit the expected highly radiogenic Pb signatures (Figure 2). In addition, some of the sediments eroded from the Lesser Himalaya have Pb isotopic compositions similar to those derived from the Tethyan Sedimentary Series and the High Himalayan Crystalline units but different Nd and Hf isotopic compositions [*Galy and France-Lanord*, 2001; *Richards et al.*, 2005; *Singh et al.*, 2008; *Garçon et al.*, 2011; *Garçon*, 2012]. These observations lead us to conclude that Pb isotopes of river sediments do not faithfully reflect that of their sources.

Sediments collected in the floodplain also define a large range of Pb isotopic compositions (Figure 2). This is in sharp contrast with their uniform Nd isotopic compositions [*Galy and France-Lanord*, 2001; *Singh et al.*, 2008; *Garçon et al.*, 2011; *Garçon*, 2012] indicating that Himalayan detritus is well homogenized before entering the floodplain and that the tributaries along the river course do not supply new material. It is therefore extremely unlikely that the Pb isotopic variations defined by sediments are due to source variability. The histogram shown in Figure 2c highlights a systematic difference between suspended load and bedload/bank sediments, the latter generally displaying more radiogenic $^{206}Pb/^{204}Pb$ ratios.

The most straightforward explanation is that the observed variability of Pb isotopes results from fluvial processes occurring during sediment transport and deposition.

Figure 3 shows the Pb isotopic compositions of the mineral separates together with the grain-size fractions. Data for these samples are provided in Supplementary Table 2. Except for titanite, all pure mineral separates lie at the lower end of the trend defined by the Himalayan sediments (Figure 3). The same is true for the clay fractions (<2μm). In contrast, the 2-50μm and 50-63μm fractions from BGP 6 and, more importantly, the heavy mineral fraction from BR 717 have extremely radiogenic Pb values and lie on the extension of the array defined by all river sediments (Figure 3). We could not measure the trace element concentrations of the heavy mineral fraction from BR 717 but petrologic observations under the binocular microscope indicate that it is highly enriched in monazite, allanite and zircon. Additionally, we note that the 2-50μm and 50-63μm fractions from BGP 6 have very high REE, Zr and Hf contents (see Supplementary Table 2), a feature indicating the presence of high amount of monazite, allanite and zircon. We thus suggest that the elevated Pb isotopic ratios of the heavy mineral separate from BR 717 and the 2-50μm and 50-63μm fractions from BGP 6 result from the presence of high proportions of zircon, monazite and allanite. We can estimate the proportion of heavy mineral present in these samples using the Hf content of zircon, the REE content of monazite and allanite (see Supplementary Table 2) and the Hf and REE contents of the <2 μm fraction from BGP 6 which, we assume, contains negligible zircon, monazite and allanite. Such a calculation shows that the two grain-size fractions from BGP 6 contain up to 2.4 wt% zircon and 0.8 wt% monazite and allanite. Due to their chemical stability and their very high U/Pb and Th/Pb ratios (See Supplementary Table 2), old zircon, monazite and allanite accumulate vast amounts of radiogenic Pb through time and their isotopic ratios become extremely radiogenic compared to most terrestrial rocks and minerals. The linear trend displayed by Himalayan river sediments in Figure 2 is thus likely due to a

"heavy mineral effect" caused by mineralogical sorting during sediment transport and deposition. In other words, the array seen in Figure 2 results from mixing between extremely radiogenic minerals (zircon, monazite and allanite) and a more subdued end member corresponding to the heavy mineral-free component of the Himalayan crust.

We defined the composition of the heavy mineral-free component (pink star in Figure 3) by averaging the Pb isotopic composition of all heavy-mineral-poor samples (clay fractions <2μm) together with that of the pure K-feldspar separate because K-feldspar hosts most of the Pb present in crustal rocks together with very little U and Th [*Patterson and Tatsumoto*, 1964; *Hemming and McLennan*, 2001]. The Pb isotopic composition of the radiogenic heavy-mineral end-member cannot be precisely constrained using the values measured in our heavy mineral fraction because this fraction contains large amounts of monazite, allanite and zircon but it also includes garnet and epidote that significantly lower its bulk Pb isotopic composition. The Pb isotopic composition of the pure radiogenic heavy-mineral end-member was thus estimated using the Pb contents, the isotopic compositions and the estimated heavy mineral content (3.2wt%) of samples BGP 6 B and BGP 6 C (see Supplementary Table 2). We expect its composition to slightly vary depending on the relative proportions of zircon, monazite and allanite in the assemblage but, given the very radiogenic composition of these minerals, such variations should not create much scatter at the lower end of the mixing line. The resulting mixing lines are shown in Figures 3 and 4.

Observations supporting our "heavy mineral effect" interpretation are:

(1) Our calculation demonstrates that less than 1wt% of extremely radiogenic minerals (zircon, monazite and allanite) added to the non-radiogenic component is enough to explain the entire range of Pb isotopic values measured for Himalayan river sediments (Figures 4a & c). Such proportions are consistent with the proportion determined independently by *Garzanti et al.*[2010, 2011] in sediments from the Ganga in Bangladesh.

(2) Radiogenic Pb in zircon, monazite and allanite explains why bedloads have more radiogenic Pb isotopes than suspended loads (Figure 2c). Mineral sorting during sediment transport enriches bedloads in fast-settling coarse and dense minerals, such as zircons, monazites and allanites, whereas suspended loads are preferentially enriched in platy phyllosilicates and other slow-setting minerals.

(3) The slope of the array defined by all sediments in $^{207}Pb/^{204}Pb$ vs. $^{206}Pb/^{204}Pb$ isotopic space (Figure 2a) is totally controlled by the very radiogenic isotopic signature of the heavy mineral fraction, and it provides an age of 1.6±0.1 Ga. This age is consistent with the average U-Pb age of 1.7 Ga that we calculated using data published by *DeCelles et al.*[1998] on detrital zircons from modern Himalayan rivers. We are therefore confident that the array defined by Himalayan river sediments in Pb isotopic spaces represents the varying contribution of heavy minerals in the sedimentary materials.

We can take the argument further and use our data to estimate the average Pb isotopic composition of the upper Himalayan crust provided that the lead present in sediments is representative of its crustal source. In rivers, most Pb is transported in solid loads (i.e. suspended and bed loads) but some is also present as dissolved phase. Considering the average Pb concentration of river sediments given by *Viers et al.*[2009] (i.e. 61 ppm) and the average worldwide sediment flux of *Hay et al.*[1998] (i.e. $20x10^{12}$ $kg.y^{-1}$), we estimate that about 1200 kt of sediment Pb reach the world ocean each year. By contrast, *Gaillardet et al.*[2003] calculated that only 3 $kt.yr^{-1}$ of dissolved Pb are delivered into the world ocean. This means that the amount of Pb transferred from continent to ocean in a dissolved form is very small compared to the amount of Pb initially present in crustal rocks submitted to weathering. Lead present in suspended and bed loads thus likely reflects the composition of the upper crust provided that a correction for the "heavy mineral effect" is made. We are

therefore confident that the average Pb isotopic composition of the upper Himalayan crust can be evaluated using our Pb data.

Assuming that all Zr in the upper continental crust (i.e. 193 ppm after *Rudnick and Gao* [2003]) resides in zircon, and all its REE (i.e. 148 ppm after *Rudnick and Gao* [2003]) in monazite and allanite, we estimate that crustal rocks contain a maximum of 0.03wt% of zircon and 0.04wt% of monazite and allanite. With these proportions, mixing calculations indicate that the average Pb isotopic composition of the upper Himalayan crust is, within error, similar to our unradiogenic end member (pink star in Figures 3 and 4). This value is less radiogenic than the average Pb composition of the Himalayan-derived suspended loads, bedloads and bank sediments (Figure 2c), indicating that river sediments are more radiogenic than their sources due to the "heavy mineral effect". In addition, it suggests that zircon, monazite and allanite are not restricted to the bedload but are also present in fine suspended load, either as small individual grains or as inclusions in other minerals (e.g. phyllosilicates). Consequently, we believe that Pb isotopic variability of sediments cannot be used as a proxy for source and/or anthropogenic changes unless mineralogical effects are carefully evaluated and corrected for. Finally, we emphasize that the "heavy mineral effect" is particularly visible in the Himalayan sediments because the detrital heavy minerals being relatively old, their extremely radiogenic Pb isotopic compositions can easily influence the bulk sediment Pb isotopic budget. Of course, a smaller effect is expected if the mean age of the eroded sources is younger.

4.2. New value for the average upper continental crust Pb isotopic composition

At a more global scale, we evaluate the Pb isotopic composition of the upper continental crust following the two-stage approach of *Asmerom and Jacobsen*[1993] using our Pb isotopic values and an average extraction age for the Himalayan crust from the mantle.

The average extraction age of the Himalayan crust is constrained using the average Nd model age of Himalayan river sediments i.e. 2.2±0.1 (1σ) Ga calculated using the Nd data published by *Singh et al.* [2008], *Garçon et al*.[2011] and *Garçon* [2012]. Using this Nd model age and its associated uncertainties, we obtain a mantle-stage μ_1 value ($^{238}U/^{204}Pb$) of 8.40 ± 0.02 (1σ) followed by a crustal-stage μ_2 value of 11.6 ± 0.2 (1σ) (see Figure 4), values that are in complete agreement with those commonly suggested for mantle and upper continental crust [*Asmerom and Jacobsen*, 1993; *Kramers and Tolstikhin*, 1997]. A similar calculation for κ_1 and κ_2 values ($^{232}Th/^{238}U$) using $^{208}Pb/^{204}Pb$ ratios is unconstrained because the two κ values are interdependent, but κ is, on average, around 4.0. Using our μ_1 and μ_2 values and κ values of 4.0, we can calculate the Pb isotopic composition of upper continental crust as a function of its average extraction time from the mantle (Table 1). Nd model ages suggested for average upper continental crust range between 1.5 and 2.2 Ga [*Goldstein and Jacobsen*, 1988; *Jacobsen*, 1988] and can be used to estimate the average crustal Pb isotopic composition. For an upper crust with an average age of 1.5 Ga, the $^{206}Pb/^{204}Pb$ ratio is 18.76 and it increases to 19.24 for an average age of 2.2 Ga as shown by the black line in Figure 4b and 4d. Using the commonly accepted average value of 1.8 Ga for the upper crust, we suggest the following Pb values: $^{206}Pb/^{204}Pb$=18.96±0.06(1σ), $^{207}Pb/^{204}Pb$=15.73±0.02(1σ) and $^{208}Pb/^{204}Pb$=39.16±0.06 (1σ) (Table 1). If, in the future, a different average age for crust differentiation is established using independent methods, another value can be easily calculated.

Our suggested $^{206}Pb/^{204}Pb$ ratio for the upper crust is always displaced to the left of former estimates in Figure 4b notwithstanding whether they are based on Pb evolution models [*Kramers and Tolstikhin, 1997*; *Zartman and Doe*, 1981] or on suspended river sediments [*Asmerom and Jacobsen*, 1993; *Millot et al.*, 2004] (Table 1). We believe that the literature values derived from river sediments are too high because they do not take into account the "heavy mineral effect" on Pb isotopes. Our Pb estimate is also less radiogenic than that of

Hemming and McLennan [2001] which is based on deep-sea turbidite data (Figure 4). The difference might be attributed to addition of labile lead in the marine environment due to the very short residence time of dissolved lead in seawater. However, marine hydrogenous sediments such as ferromanganese crusts have crustal-like Pb isotopic compositions (i.e. 18.6-19.3 for $^{206}Pb/^{204}Pb$ ratios, 15.6-15.7 for $^{207}Pb/^{204}Pb$ ratios and 38.6-39.5 for $^{208}Pb/^{204}Pb$ ratios, *von Blanckenburg et al.*[1996]) and addition of such lead cannot explain the observed difference between the two estimates. Instead, we think that since turbidites are coarse-grained sediments containing relatively high amount of heavy minerals, their Pb values are also shifted towards too radiogenic values due to a "heavy mineral effect".

Our estimate strongly resembles the average composition of global subducting sediments [*Plank*, 2013] (Figure 4) demonstrating that on average material recycled back into the mantle through subduction zones is not affected by the "heavy mineral effect" and has the same Pb isotopic composition as the upper continental crust. Finally, our Pb estimate for the upper crust still lies on the right on the 4.55 Ga geochron i.e. the meteorite isochron on which the Earth as a whole is expected to plot (Figure 4), a shift called the first Pb paradox [*Allègre,* 1969]. Our new Pb values do not resolve this Pb paradox, confirming that an unradiogenic lead reservoir is still needed to balance the radiogenic composition of the upper continental crust.

5. CONCLUSIONS

Our results clearly show that Pb isotopes of river sediments are biased by a "heavy mineral effect" caused by mineral sorting processes during fluvial transport. Both bedloads and suspended loads have Pb isotopic compositions more radiogenic than their source rocks due to the presence of a few but extremely radiogenic zircons, monazites and allanites. Consequently, Pb isotopic variability of sediments cannot be used as a proxy for source

and/or anthropogenic changes unless mineralogical effects are carefully evaluated and corrected for. We suggest that estimates of the average Pb isotopic composition of the eroded crust should be preferentially evaluated using Pb-rich K-feldspars separates and/or clay fractions rather than bulk sediment. After correction of the "heavy mineral effect", we establish a new Pb isotopic value for the upper continental crust.

ACKNOWLEDGEMENTS

We thank A. Galy, V. Galy and M. Lupker for sediment sampling, S. Andò for his help during mineral separations, S. Bureau for her help in the clean lab, P. Telouk for assistance during MC-ICP-MS measurements at Lyon and N.T. Arndt for constructive discussions that helped improving the style and content of the manuscript. We are also grateful to B.S. Kamber, an anonymous reviewer and the editor L. Derry for their constructive comments that greatly improved the content of the discussion. This study was supported by funding from CNRS and INSU programs.

REFERENCES

Allègre, C. J. (1969), Comportement des systèmes U-Th-Pb dans le manteau supérieur et modèle d'évolution de ce dernier au cours des temps géologiques, *Earth and Planetary Science Letters*, *5*, 261–269.

Allègre, C. J., B. Dupré, P. Négrel, and J. Gaillardet (1996), Sr-Nd-Pb isotope systematics in Amazon and Congo River systems: constraints about erosion processes, *Chemical Geology*, *131*(1), 93–112.

Asmerom, Y., and S. B. Jacobsen (1993), The Pb isotopic evolution of the Earth: inferences from river water suspended loads, *Earth and Planetary Science Letters*, *115*(1-4), 245–256.

Chauvel, C., S. Bureau, and C. Poggi (2011), Comprehensive chemical and isotopic analyses of basalt and sediment reference materials, *Geostandards and Geoanalytical Research*, *35*(1), 125–143.

DeCelles, P., G. Gehrels, J. Quade, B. LaReau, and M. Spurlin (2000), Tectonic implications of U-Pb zircon ages of the Himalayan orogenic belt in Nepal, *Science*, *288*(5465), 497–499.

DeCelles, P., G. Gehrels, J. Quade, T. Ojha, P. Kapp, and B. Upreti (1998), Neogene foreland basin deposits, erosional unroofing, and the kinematic history of the Himalayan fold-thrust belt, western Nepal, *Geological Society of America Bulletin*, *110*(1), 2–21.

Gaillardet, J., J. Viers, and B. Dupré (2003), Trace Elements in River Waters, in *Treatise on Geochemistry Vol.5 Surface and Ground Water, Weathering, and Soils*, pp. 225–272, Elsevier.

Galer, S. J. G., and W. Abouchami (1998), Practical application of lead triple spiking for correction of instrumental mass discrimination, *Mineralogical Magazine*, 491–492.

Galy, V., C. France-Lanord, and B. Lartiges (2008), Loading and fate of particulate organic carbon from the Himalaya to the Ganga–Brahmaputra delta, *Geochimica et Cosmochimica Acta*, *72*, 1767–1787.

Galy, A., and C. France-Lanord (2001), Higher erosion rates in the Himalaya: Geochemical constraints on riverine fluxes, *Geology*, *29*(1), 23–26.

Garçon, M. (2012), Variabilité chimique et isotopique causée par les processus sédimentaires dans les sédiments de rivières Himalayennes, *PhD Thesis, Grenoble University, France*.

Garçon, M., C. Chauvel, and C. France-Lanord (2011), Large Nd-Hf isotopic decoupling in Himalayan River Sediments, *AGU Fall Meeting Abstracts*, *-1*, 0610.

Garzanti, E., S. Andò, C. France-Lanord, G. Vezzoli, P. Censi, V. Galy, and Y. Najman (2010), Mineralogical and chemical variability of fluvial sediments 1. Bedload sand (Ganga–Brahmaputra, Bangladesh), *Earth and Planetary Science Letters*, *299*(3-4), 368–381.

Garzanti, E., S. Andò, C. France-Lanord, P. Censi, Pietro Vignola, V. Galy, and M. Lupker (2011), Mineralogical and chemical variability of fluvial sediments 2. Suspended-load silt (Ganga–Brahmaputra, Bangladesh), *Earth and Planetary Science Letters*, *302*(1-2), 107–120.

Goldstein, S., and S. B. Jacobsen (1988), Nd and Sr isotopic systematics of river water suspended material: implications for crustal evolution, *Earth and Planetary Science Letters*, *87*, 249–265.

Hay, W. W. (1998), Detrital sediment fluxes from continents to oceans, *Chemical Geology*, *145*(3), 287–323.

Hemming, S., and S. McLennan (2001), Pb isotope compositions of modern deep sea turbidites, *Earth and Planetary Science Letters*, *184*(2), 489–503.

Jacobsen, S. B. (1988), Isotopic constraints on crustal growth and recycling, *Earth and Planetary Science Letters*, *90*(3), 315–329.

Kramers, J. D., and I. N. Tolstikhin (1997), Two terrestrial lead isotope paradoxes, forward transport modelling, core formation and the history of the continental crust, *Chemical Geology*, *139*(1), 75–110.

Le Fort, P. (1975), Himalayas: the collided range. Present knowledge of the continental arc,

American Journal of Science, 275A, 1-44.

Lupker, M., C. France-Lanord, J. lavé, J. Bouchez, V. Galy, F. Métivier, J. Gaillardet, B. Lartiges, and J.-L. Mugnier (2011), A Rouse-based method to integrate the chemical composition of river sediments: Application to the Ganga basin, *J. Geophys. Res.*, *116*(F4), F04012.

Lupker, M., C. France-Lanord, V. Galy, J. lavé, J. Gaillardet, A. P. Gajurel, C. Guilmette, M. Rahman, S. K. Singh, and R. Sinha (2012), Predominant floodplain over mountain weathering of Himalayan sediments (Ganga basin), *Geochimica et Cosmochimica Acta*, *84*(C), 410–432.

Milliman, J., and R. H. Meade (1983), World-wide delivery of river sediment to the oceans, *The Journal of Geology*, *91*(1), 1–21.

Millot, R., C. J. Allègre, J. Gaillardet, and S. Roy (2004), Lead isotopic systematics of major river sediments: a new estimate of the Pb isotopic composition of the Upper Continental Crust, *Chemical Geology*, *203*(1), 75–90.

Parrish, R. R., and V. Hodges (1996), Isotopic constraints on the age and provenance of the Lesser and Greater Himalayan sequences, Nepalese Himalaya, *Geological Society of America Bulletin*, *108*(7), 904–911.

Patchett, P. J., W. M. White, H. Feldmann, S. Kielinczuk, and A. W. Hofmann (1984), Hafnium/rare earth element fractionation in the sedimentary system and crustal recycling into the Earth's mantle, *Earth and Planetary Science Letters*, *69*, 365–378.

Patterson, C., and M. Tatsumoto (1964), The significance of lead isotopes in detrital feldspar with respect to chemical differentiation within the earth's mantle, *Geochimica et Cosmochimica Acta*, *28*(1), 1–22.

Plank, T. (2013, in press), The Chemical Composition of Subducting Sediments, *in The Crust edited by Rudnick, R. L., in Treatise on Geochemistry*, *Vol.3, 1st edt, edited by Holland, H. D., and K. K. Turekian, Elsevier-Pergamon, Oxford,* doi:10.1016/B978-0-08-095975-7.00319-3

Richards, A., T. Argles, N. Harris, R. Parrish, T. Ahmad, F. Darbyshire, and E. Draganits (2005), Himalayan architecture constrained by isotopic tracers from clastic sediments, *Earth and Planetary Science Letters*, *236*(3), 773–796.

Rudnick, R. L., and S. Gao (2003), Composition of the Continental Crust, *in The Crust edited by Rudnick, R. L., in Treatise on Geochemistry*, *Vol.3, 1st edt, edited by Holland, H. D., and Turekian K. K., Elsevier-Pergamon, Oxford.*

Singh, S. K., S. K. Rai, and S. Krishnaswami (2008), Sr and Nd isotopes in river sediments from the Ganga Basin: Sediment provenance and spatial variability in physical erosion, *J. Geophys. Res.*, *113*(F3), F03006.

Stacey, J. S., and J. D. Kramers (1975), Approximation of terrestrial lead isotope evolution by a two-stage model, *Earth and Planetary Science Letters*, *26*(2), 207–221.

Tatsumoto, M., R. J. Knight, and C. J. Allègre (1973), Time differences in the formation of

meteorites as determined from the ratio of lead-207 to lead-206, *Science 180, 1279-1283*.

Viers, J., B. Dupré, and J. Gaillardet (2009), Chemical composition of suspended sediments in World Rivers: New insights from a new database, *Science of the Total Environment*, *407*(2), 853–868, doi:10.1016/j.scitotenv.2008.09.053.

von Blanckenburg F., R. K. O'nions, and J. R. Heinz (1996), Distribution and sources of pre-anthropogenic lead isotopes in deep ocean water from Fe-Mn crusts, *Geochimica et Cosmochimica Acta*, *60*(24), 4957–4963.

White, W. M., F. Albarède, and P. Télouk (2000), High-precision analysis of Pb isotope ratios by multi-collector ICP-MS, *Chemical Geology*, *167*(3), 257–270.

Zartman, R. E., and B. R. Doe (1981), Plumbotectonics-the model, *Tectonophysics*, *75*(1-2), 135–162.

TABLE CAPTION

Table 1: Our Pb estimates for average upper continental crust

Our Pb estimates were calculated using $\mu_1 = 8.40$, $\mu_2 = 11.6$ and $\kappa_1 = \kappa_2 = 4.0$ from the isotope ratios of primeval Pb of Canyon Diablo as published by *Tatsumoto et al*.[1973]. Our preferred values are indicated in bold and correspond to an average age of 1.8 Ga for the upper crust. Average Pb isotopic values for the upper continental crust estimated by other studies [*Zartman and Doe*, 1981; *Asmerom and Jacobsen*, 1993; *Kramers and Tolstikhin*, 1997; *Hemming and McLennan*, 2001; *Millot et al.*, 2004] are also reported for comparison.

FIGURE CAPTIONS

Figure 1: Map of the Ganga fluvial system

Colored stars indicate the sampling locations in the floodplain of river sediments analyzed in this study. White and grey stars indicate locations of river sediments sampled in monolithologic catchments in the mountain range. White stars: sampling sites for the Lesser Himalaya-derived sediments. Light grey stars: sampling sites for the High Himalayan Crystalline-derived sediments. Dark grey stars: sampling sites for the Tethyan Sedimentary

Series-derived sediments. See Supplementary Tables 1 and 2 for additional information on the location and nature of samples.

Figure 2: Pb isotopic compositions of Himalayan river sediments

a. $^{207}Pb/^{204}Pb$ versus $^{206}Pb/^{204}Pb$ and **b.** $^{208}Pb/^{204}Pb$ versus $^{206}Pb/^{204}Pb$ diagrams for the river sediments analyzed in this study. **c.** Histogram of $^{206}Pb/^{204}Pb$ ratios for sediments sampled in the floodplain (Ganga, Narrayani, Karnali, and Kosi Rivers).

Figure 3: Pb isotopic compositions of mineral separates and grain-size fractions.

The top two panels (**a** and **b**) show the entire range of measured isotopic compositions and the lower panels (**c**, **d**, **e** and **f**) show the position of data points at more detailed scales. The field for Himalayan river sediments corresponds to the data shown in Figure 2. The grey lines show the best linear regressions for Himalayan sediments alone. These regression lines pass through the radiogenic compositions of the two grain-size fractions and the heavy mineral concentrate shown in panels **a**, **b**, **c** and **d** and cannot be distinguished from a binary mixing line between the calculated heavy mineral end member and the unradiogenic component. Titanite is the only phase to significantly deviate from this regression. Ticks on the grey lines show the proportion of heavy minerals (zircon+monazite+allanite) in a binary mixing between our unradiogenic upper Himalayan crust estimate (pink star; $^{206}Pb/^{204}Pb$=19.24; $^{207}Pb/^{204}Pb$=15.80; $^{208}Pb/^{204}Pb$=39.51) and the calculated radiogenic heavy mineral end member (not shown in this figure, $^{206}Pb/^{204}Pb$=873; $^{207}Pb/^{204}Pb$=96; $^{208}Pb/^{204}Pb$=837, see Supplementary Table 2).

Figure 4: Pb isotopic diagrams comparing our estimated composition of the upper continental crust and other published values.

UCC: Upper continental crust. Pink dots represent the Himalayan river sediments as shown in Figure 2. **a. c.** Fields for Ocean Island Basalts (OIB) and Mid-Ocean Ridge Basalts (MORB) show the Pb isotopic variability of the Earth's mantle. These fields were constructed using data from GEOROC and PETDB databases. **b. d.** Blow-up showing the average Pb isotopic composition of the upper continental crust as a function of its mean age (T). Our preferred value is shown with a black star and corresponds to a mean age of 1.8 Ga. Other Pb estimates [*Stacey and Kramers*, 1975; *Zartman and Doe*, 1981; *Asmerom and Jacobsen*, 1993; *Kramers and Tolstikhin*, 1997; *Hemming and McLennan*, 2001; *Millot et al.*, 2004; *Plank*, 2013] are also shown for comparison. The GLOSS II estimate in panel **d.** is behind the black star.

Table 1: Pb isotopic estimates for the upper continental crust

Source	Methods used to estimate Pb isotopic values	Average Model age (Ga)	$^{208}Pb/^{204}Pb$		$^{207}Pb/^{204}Pb$		$^{206}Pb/^{204}Pb$	
This study	Calculated using $\mu_1 = 8.40$, $\mu_2 = 11.6$ and $\kappa_1 = \kappa_2 = 4.0$ from the isotope ratios of primeval Pb of Canyon Diablo	1.5	39.00	± 0.06	15.69	± 0.02	18.76	± 0.05
		1.8 (preferred)	**39.21**	**± 0.06**	**15.73**	**± 0.02**	**18.95**	**± 0.06**
		2.0	39.36	± 0.07	15.76	± 0.02	19.09	± 0.06
		2.2	39.51	± 0.07	15.80	± 0.02	19.24	± 0.06
Asmerom and Jacobsen (1993)	Average composition of river suspended loads		39.33	± 0.39	15.76	± 0.09	19.32	± 0.07
Hemming and McLennan (2001)	Average composiiton of turbidites and river sediments		39.58		15.78		19.22	
Millot et al. (2004)	Average composition of river sediments balanced by sediment flux		39.35		15.74		19.07	
	Average composition of river sediments balanced by surface area		39.03		15.71		18.93	
Zartman and Doe (1981)	Plumbotectonic Earth evolution model		39.06		15.73		19.33	
Kramers and Tolstikhin (1997)	Earth evolution model		39.32		15.71		19.17	

Figure 1

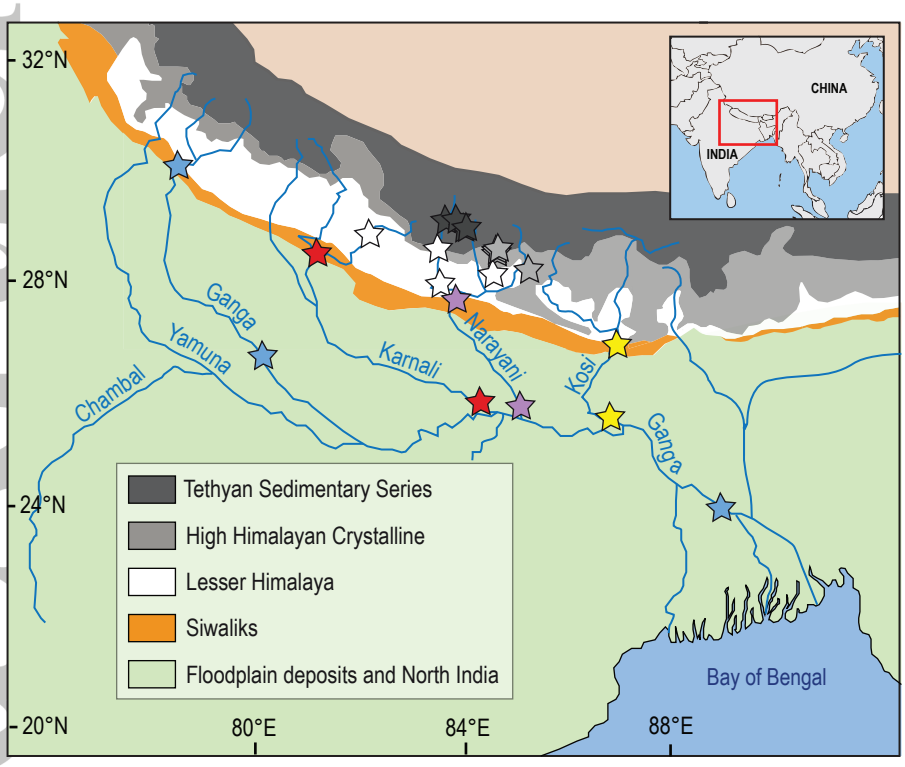

Figure 2

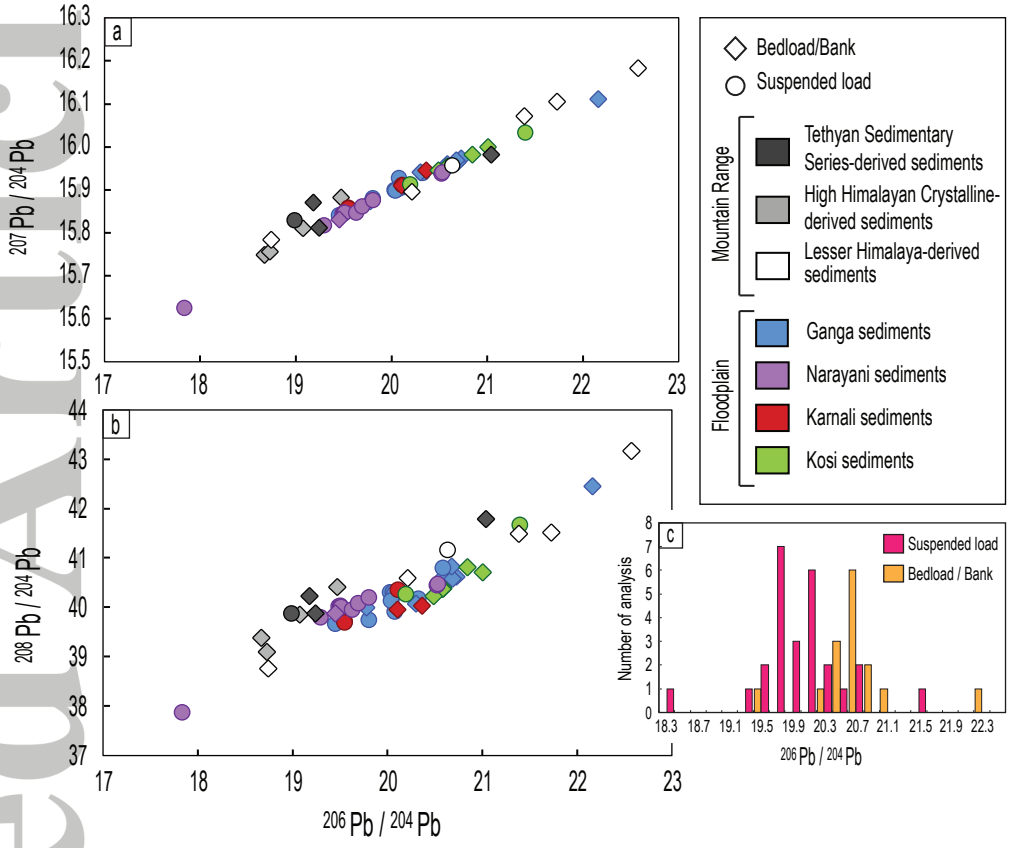

Figure 3

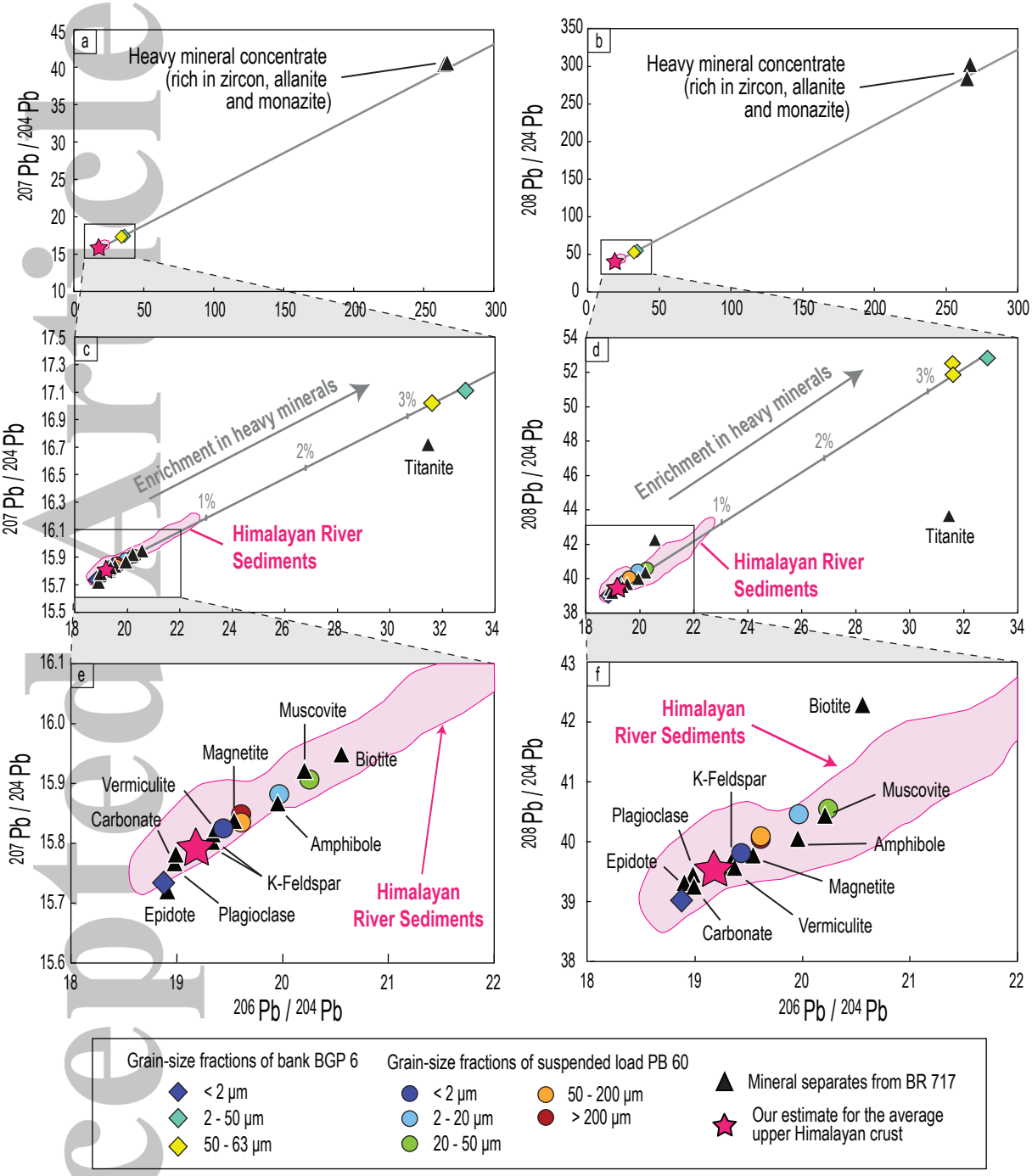

Figure 4

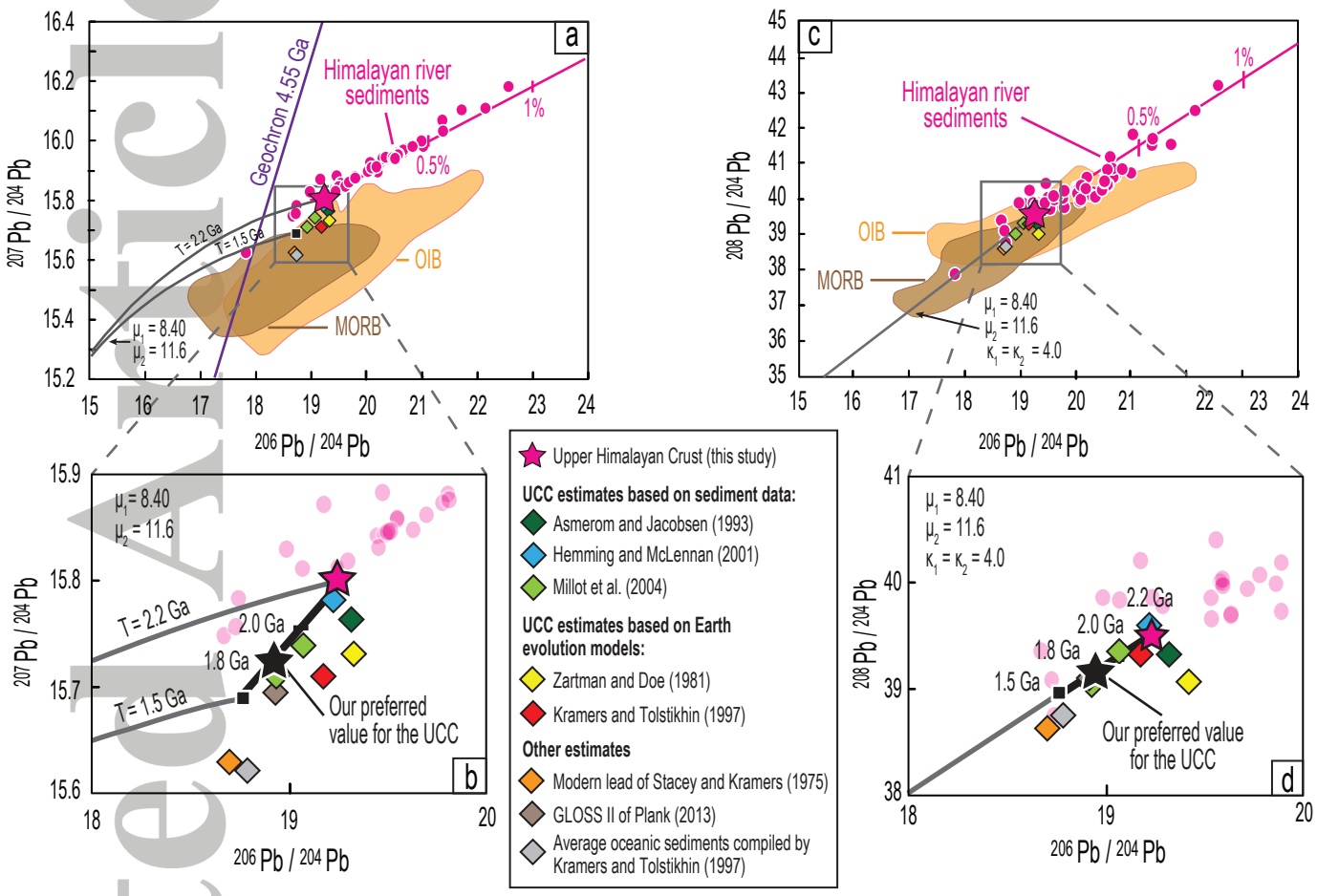

Supplementary Table 1: Pb isotopes in sediments

From rivers draining monolithologic basins in the Himalayan range

Sample Name	Locality	River	Type of sediment	Pb (ppm)	$^{208}Pb/^{204}Pb$	2σ	$^{207}Pb/^{204}Pb$	2σ	$^{206}Pb/^{204}Pb$	2σ
Lesser Himalaya units										
R 94-12	Sarmi, Nepal	Tributary of the Bheri River	Bedload	87.1	40.5828	0.0020	15.8958	0.0007	20.2112	0.0009
MO 102	Confluence Darondi/Marsel Khola, Nepal	Marsel Khola	Bank sediment	12.4	41.4861	0.0019	16.0709	0.0008	21.3862	0.0009
MO 102 re-run					41.4857	0.0025	16.0701	0.0009	21.3858	0.0011
MO 112	Confluence Bhuri Gandaki/Isul Khola, Nepal	Isul Khola	Bank sediment sediment, gravel sample	9.19	43.1638	0.0034	16.1832	0.0014	22.5753	0.0016
PB 33	Nepal	Ghara khola	Suspended Load	17.1	41.1620	0.0021	15.9564	0.0008	20.6345	0.0009
PB 37	Nepal	Beg Khola	Bank sediment sediment	11.6	38.7584	0.0023	15.7833	0.0009	18.7442	0.0007
MO 207	Waling, Nepal	Andi Khola	Bedload	9.12	41.5076	0.0038	16.1047	0.0013	21.7295	0.0017
High Himalayan Crystalline units										
MO 73	Nepal	Tributary of the Chepe khola	Bank sediment	8.94	40.4110	0.0033	15.8820	0.0013	19.4708	0.0011
MO 50	Nepal	Chepe khola	Bank sediment	15.1	39.3746	0.0030	15.7486	0.0010	18.6711	0.0009
MO 59	Nepal	Chepe khola	Bank sediment	23.3	39.0933	0.0036	15.7565	0.0013	18.7296	0.0015
KN 83	Ghyangphedi, Nepal	Tadi khola	Bedload	17.9	39.8509	0.0018	15.8109	0.0006	19.0735	0.0006
Tethyan Sedimentary Series										
MO 504	Tukche, Nepal	Yamkim khola	Suspended Load	33.9	39.8670	0.0022	15.8287	0.0008	18.9871	0.0008
NAG 22	Pedi, Nepal	Marsyandi (10 km away from the River Source)	Bedload	235	41.7816	0.0020	15.9819	0.0006	21.0408	0.0007
MAR-50	Temang, Nepal	Marsyandi (60 km away from the River Source)	Bedload	20.9	39.8665	0.0031	15.8117	0.0011	19.2416	0.0013
MAR-40	Sabche, Nepal	Sabche khola	Bedload	35.2	40.2185	0.0034	15.8706	0.0011	19.1799	0.0012
MAR-40 re-run					40.2139	0.0034	15.8676	0.0012	19.1795	0.0013

From the Ganga river and its major tributaries in the floodplain

Sample Name	Locality	Approximative distance from River Source (km)	Type of sediment	Pb (ppm)	$^{208}Pb/^{204}Pb$	2σ	$^{207}Pb/^{204}Pb$	2σ	$^{206}Pb/^{204}Pb$	2σ
Ganga River										
BR 931	Devrapayag, India	260	Suspended Load	29.2	39.6694	0.0037	15.8417	0.0012	19.4498	0.0013
BR 932	Devrapayag, India	260	Suspended Load	21.0	40.1668	0.0040	15.9401	0.0013	20.3250	0.0014
BR 922	Rishikesh, India	260	Suspended Load	29.1	39.9124	0.0037	15.9272	0.0014	20.0784	0.0013
BR 924	Rishikesh, India	260	Bank sediment	21.4	40.0740	0.0028	15.9405	0.0009	20.3010	0.0010
BR 943	Kanpur, India	800	Suspended Load	23.5	39.7368	0.0028	15.8813	0.0009	19.8032	0.0009
BR 946	Kanpur, India	800	Bedload	18.9	40.5941	0.0031	15.9605	0.0010	20.5807	0.0011
BGP 6	Rajshahi, India	2570	Bank sediment	17.8	40.6213	0.0043	15.9733	0.0014	20.7277	0.0014
BGP 6 Dup	Rajshahi, India	2570	Bank sediment	17.6	40.5790	0.0039	15.9644	0.0013	20.6899	0.0018
BR 415	Harding bridge, Bangladesh	2640	Suspended Load	30.4	40.3003	0.0018	15.8991	0.0006	20.0301	0.0007
BR 415 re-run					40.2903	0.0021	15.8958	0.0008	20.0256	0.0007
BR 414	Harding bridge, Bangladesh	2640	Suspended Load	26.2	40.3019	0.0025	15.9013	0.0005	20.0574	0.0009
BR 413	Harding bridge, Bangladesh	2640	Suspended Load	25.3	40.2931	0.0034	15.9040	0.0007	20.0912	0.0008
BR 412	Harding bridge, Bangladesh	2640	Suspended Load	25.3	40.2725	0.0016	15.9040	0.0006	20.0756	0.0007

Sample Name	Locality	Approximative distance from River Source (km)	Type of sediment	Pb (ppm)	$^{208}Pb/^{204}Pb$	2σ	$^{207}Pb/^{204}Pb$	2σ	$^{206}Pb/^{204}Pb$	2σ
BR 411	Harding bridge, Bangladesh	2640	Suspended Load	17.4	40.1312	0.0028	15.8984	0.0010	20.0387	0.0011
BR 418	Harding bridge, Bangladesh	2640	Bedload	15.0	40.8292	0.0023	15.9684	0.0009	20.6767	0.0009
BR 8252	Harding bridge, Bangladesh	2640	Bedload	10.7	40.8030	0.0026	15.9548	0.0009	20.5845	0.0010
BR 8253	Harding bridge, Bangladesh	2640	Suspended Load	10.5	39.9963	0.0028	15.8730	0.0013	19.7765	0.0010
BR 717	Harding bridge, Bangladesh	2640	Bedload	14.2	42.4525	0.0027	16.1109	0.0009	22.1618	0.0010
Karnali River										
PB 79	Chisapani, Nepal	260	Suspended Load	12.7	40.3508	0.0033	15.9117	0.0012	20.1105	0.0011
PB 80	Chisapani, Nepal	260	Bank sediment	13.9	39.9552	0.0033	15.9101	0.0010	20.1047	0.0011
BR 8113	Revelganj, India	850	Suspended Load	30.3	39.7131	0.0028	15.8585	0.0010	19.5477	0.0012
BR 8113 Dup	Revelganj, India	850	Suspended Load	30.5	39.6936	0.0030	15.8570	0.0007	19.5474	0.0010
Kosi River										
LO 762	Chatara, Nepal	180	Suspended Load	17.8	40.2696	0.0045	15.9136	0.0014	20.1936	0.0010
LO 762 re-run					40.2771	0.0046	15.9163	0.0013	20.1914	0.0017
LO 763	Chatara, Nepal	180	Bank sediment	17.6	40.3778	0.0019	15.9529	0.0006	20.5899	0.0008
LO 763 Dup	Chatara, Nepal	180	Bank sediment	19.1	40.3688	0.0022	15.9535	0.0008	20.5825	0.0012
PB 69	Chatara, Nepal	440	Suspended Load	17.3	41.6645	0.0026	16.0340	0.0008	21.3982	0.0010
PB 70	Chatara, Nepal	440	Bank sediment	15.3	40.7029	0.0027	15.9993	0.0009	21.0066	0.0010
BR 331	Dumarighat, India	440	Bank sediment	15.7	40.8060	0.0026	15.9820	0.0009	20.8453	0.0010
BR 332	Dumarighat, India	440	Bank sediment	17.2	40.2245	0.0028	15.9449	0.0011	20.4868	0.0011
Narayani River										
LO 757	Narayanghat, Nepal	200	Suspended Load	24.8	40.0158	0.0014	15.8437	0.0004	19.4858	0.0005
LO 756	Narayanghat, Nepal	200	Suspended Load	72.0	37.8642	0.0026	15.6249	0.0009	17.8352	0.0009
LO 756 re-run					37.8540	0.0031	15.6222	0.0012	17.8336	0.0011
LO 754	Narayanghat, Nepal	200	Suspended Load	23.6	40.0035	0.0021	15.8452	0.0006	19.5028	0.0008
LO 755	Narayanghat, Nepal	200	Suspended Load	24.1	40.0317	0.0018	15.8467	0.0006	19.5035	0.0007
LO 755 Dup	Narayanghat, Nepal	200	Suspended Load	25.0	40.0043	0.0036	15.8468	0.0007	19.5100	0.0007
LO 758 C	Narayanghat, Nepal	200	Suspended Load	15.5	39.9544	0.0026	15.8476	0.0010	19.6294	0.0010
PB 54	Narayanghat, Nepal	200	Suspended Load	19.3	40.0753	0.0020	15.8614	0.0015	19.6925	0.0016
PB 60	Narayanghat, Nepal	200	Suspended Load	16.6						
LO 1002	Narayanghat, Nepal	200	Suspended Load	27.4	39.7958	0.0049	15.8183	0.0009	19.2935	0.0010
LO 1007	Narayanghat, Nepal	200	Suspended Load	13.6	40.4425	0.0025	15.9385	0.0009	20.5219	0.0009
LO 1007 Dup	Narayanghat, Nepal	200	Suspended Load	12.2	40.4698	0.0024	15.9405	0.0008	20.5304	0.0010
BR 8106	Hajipur, India	550	Suspended Load	26.7	40.1990	0.0029	15.8760	0.0009	19.8046	0.0009
BR 8107	Hajipur, India	550	Bedload	20.9	39.8702	0.0031	15.8310	0.0008	19.4519	0.0011

Footnote: 2σ are in-run errors. Pb concentrations were measured by ICP-MS following Chauvel et al. (2011) on the same dissolutions as those used to measure Pb isotopic compositions
Dup stands for complete dissolution duplicates
Re-run stands for run duplicates

Supplementary Table 2: Pb isotopes in mineral separates from BR 717 and granulometric fractions separated from BGP 6 and PB 60

Sample Name	Type of mineral	Weight proportion in BR 717 after Garzanti et al. (2010)	Σ_{REE} (ppm)	Zr (ppm)	Hf (ppm)	Pb (ppm)	U/Pb	Th/Pb	$^{208}Pb/^{204}Pb$	2σ	$^{207}Pb/^{204}Pb$	2σ
BR 717 Msc	Muscovite	8.6	54.2	210.0	5.70	11.1	0.14	0.41	40.4282	0.0039	15.9237	0.0013
BR 717 Bio	Biotite		228	264	7.30	4.96	0.48	5.02	42.2870	0.0044	15.9514	0.0014
BR 717 Bio re-run									42.2816	0.0041	15.9486	0.0013
BR 717 Fd-K	K-Felspar	8.5	13.4	29.9	0.837	61.3	0.01	0.02	39.5826	0.0028	15.8053	0.0012
BR 717 Fd-K Dup	K-Felspar		27.5	21.9	0.658	75.1	0.01	0.05	39.6220	0.0025	15.8174	0.0010
BR 717 Plg	Plagioclase	7.1	25.7	94.4	2.56	12.6	0.06	0.19	39.4450	0.0035	15.7695	0.0013
BR 717Mag	Magnetite		96.5	265	7.01	19.1	0.19	0.71	39.7607	0.0041	15.8403	0.0014
BR 717 Ep	Epidote	1.1	374	183	4.76	46.9	0.14	0.38	39.2848	0.0035	15.7229	0.0014
BR 717 Ttn	Titanite	0.3	1713	2128	72.8	5.52	9.1	27.3	43.6704	0.0037	16.7220	0.0010
BR 717 Verm	Vermiculite		171	117	3.11	75.5	0.04	0.14	39.5411	0.0036	15.8266	0.0012
BR 717 Amp	Amphibole	1	202	539	15.5	24.1	0.31	1.00	40.0280	0.0031	15.8694	0.0012
BR 717 Carb	Carbonate		44.2	< DL	< DL	7.28	0.07	0.16	39.2442	0.0022	15.7839	0.0007
BR 717 Zrn-Mnz-All	Rich in zircon, monazite, allanite								280.299	0.063	39.9913	0.008
BR 717 Zrn-Mnz-All Dup	Rich in zircon, monazite, allanite								297.809	0.077	40.0467	0.011
BR 717 Zrn	Zircon	0.5	1348	416 415	10 171	19.3	31.7	11.4				
	Monazite		510 620 *	20 *	1 *	100 *	85 *	800 *				
	Allanite		186 240 *	215 *	9 *	30 *	20 *	567 *				
	Zircon + Monazite +Allanite					31 **			873 **		96 **	

Sample Name	Type of sediment	Grain-size fractions	Σ_{REE} (ppm)	Zr (ppm)	Hf (ppm)	Pb (ppm)	$^{208}Pb/^{204}Pb$		$^{207}Pb/^{204}Pb$	
BGP 6 A	Bank sediment	< 2 µm	485	447	12.2	95.2	39.0244	0.0029	15.7357	0.0010
BGP 6 C	Bank sediment	2 - 50 µm	3717	11954	290	24.3	52.8624	0.0048	17.1069	0.0014
BGP 6 B	Bank sediment	50 - 63 µm	3077	8328	205	20.9	52.5387	0.0047	17.0178	0.0012
BGP 6 B Dup	Bank sediment	50 - 63 µm	3024	8208	203	20.5	51.8890	0.0043	17.0196	0.0013
PB 60 A	Suspended Load	< 2 µm	190	119	3.13	67.1	39.8007	0.0035	15.8265	0.0012
PB 60 LF	Suspended Load	2 - 20 µm	178	150	3.96	23.2	40.4494	0.0033	15.8843	0.0011
PB 60 LG	Suspended Load	20 - 50 µm	218	345	9.44	18.0	40.5608	0.0042	15.9089	0.0014
PB 60 SF	Suspended Load	50 - 200 µm	126	119	3.12	17.7	40.0655	0.0047	15.8485	0.0017
PB 60 SG	Suspended Load	> 200 µm	71.3	136	3.63	15.8	40.0589	0.0036	15.8364	0.0013

Footnote: 2σ are in-run errors. Trace element concentrations were measured by ICP-MS following Chauvel et al. (2011) on the same dissolutions as those used to measure Pb isotopic compositions

BR 717 Zrn-Mnz-All is a heavy mineral concentrate (minerals with a density >3.3 $g.cm^{-3}$) separated from the 2-63 µm fraction of BR 717

DL: Detection limit

Dup: Complete dissolution duplicate

Σ_{REE} corresponds to the sum of the REE concentrations (i.e. La+Ce+Pr+Nd+Sm+Eu+Gd+Tb+Dy+Ho+Er+Yb+Lu)

* Data from Garzanti et al. (2010)

** Calculated composition for the radiogenic heavy mineral endmenber (see text for more details)